



ELSEVIER

Available online at www.sciencedirect.com

SCIENCE @ DIRECT®

Physica A 325 (2003) 547–560

PHYSICA A

www.elsevier.com/locate/physa

Size dependency of tension strength in natural fiber composites

G. Dill-Langer^a, R. Cruz Hidalgo^{b,*}, F. Kun^c, Y. Moreno^d,
S. Aicher^d, H.J. Herrmann^b

^a*Otto-Graf-Institute, University of Stuttgart, Pfaffenwaldring 4, 70569 Stuttgart, Germany*

^b*ICAI, University of Stuttgart, Pfaffenwaldring 27, 70569 Stuttgart, Germany*

^c*Department of Theoretical Physics, University of Debrecen, Debrecen, Hungary*

^d*The Abdus Salam International Centre for Theoretical Physics, Condensed Matter Group,
P.O. Box 586, Trieste, I-34014, Italy*

Received 15 January 2003

Abstract

This paper reports on a combined experimental and theoretical study on the size dependency of tension strength of clear wood at loading parallel to fiber direction. The fracture behavior of the tested softwood specimens was found to be rather brittle with low precursory activity and a statistical variation of the strength. The distribution of the strength values can be well fitted with a Weibull distribution distinguished by a shape parameter $\rho \sim 8 - 10$. A significant dependency of the mean strength of the material on the cross-sectional size of the specimens was obtained. The range of load redistribution in clear wood subjected to tension parallel to fiber was assessed by the theoretical concept of fiber bundle models for fiber composites. Hereby the macroscopic behavior was modelled in terms of the microscopic damage process.

© 2003 Elsevier Science B.V. All rights reserved.

Keywords: Wood fibers; Size effect; Fiber bundle models

1. Introduction

The material wood is a natural unidirectional fiber composite. The fibrous character of softwoods can be found at two different length scales: On the micro-scale (some 10–100 μm) softwood consists of hollow, unidirectionally aligned cells, in the following named ‘micro-fibers’, which are bonded in lateral direction by very thin

* Corresponding author.

E-mail address: raul.cruz@ica1.uni-stuttgart.de (R.C. Hidalgo).

layers of matrix material. On the ultra-scale (some 0.01–1 μm) the walls of the hollow micro-fibers consist of bundles of very stiff and strong cellulose chains (ultra-fibers), being wriggled around the axis of the micro-fibers in different layers and mainly bonded by two matrix materials, lignin and hemicellulosis. The crystalline structure of the ‘ultra-fibers’ determines the brittle character of fracture at tension loading and the very high ratios of strength and stiffness vs. density. The unidirectional build-up at the micro-scale leads to a pronounced anisotropy in the directions parallel and perpendicular to the fiber; typically strength and stiffness values differ by a factor of 10–20 for the two directions. The natural growth process forwarding several kinds of defects and irregularities yields a high scatter of all material parameters; typically coefficients of variation are in the range of 15–30 percent.

Scale effects of wood strength are well known with respect to tension loading perpendicular to fiber direction. In this weak plane of wood, exhibiting the most brittle failure mode of splitting, the pronounced scale effect of the stressed volume can be modelled adequately by a simple weakest link approach for a purely serial system [1]. However, recent investigations showed that the purely serial system approach is not fully applicable for realistic length scales but that the stress redistribution effects of partial parallel systems have to be taken into account.

In case of bending and tension parallel to fiber direction scale effects of width and depth have been reported in several studies [2]. However, modelling of wood loaded parallel to fiber as a parallel system of fibers has not yet been performed to the knowledge of the authors. Existing models mostly treat all scale effects in the view of some modified weakest link approach thereby silently neglecting the effects of stress redistribution after the initial fracture of the weakest fiber [3].

In the presented study results of tension strength of wood parallel to fiber direction obtained from quasistatistical ramp-loading are presented. As anticipated, the tested wood specimens exhibited a rather brittle fracture character with low precursory activity preceding final failure. Tension strength for the specimens of a fixed size can be described by a Weibull distribution. Furthermore, samples of larger cross-sectional dimensions have smaller average strength indicating the existence of a size effect of wood, when loaded in tension parallel to fiber direction.

In order to obtain an accurate prediction of the point of ultimate failure the statistical evolution of the damage across the entire macroscopic system and the associated stress redistributions have to be considered, being a demanding problem. One of the most important approaches to the strength and reliability of fiber composites reducing the complexity thoroughly are the Fiber bundle models (FBM). The basic concept of FBM was first introduced by Daniels [4] and Coleman [5] and in the following has been the subject to intense research efforts during the last decades [6–24]. Fiber bundle models are constructed so that a set of fibers is arranged in parallel, each one having identical elastic properties but statistically distributed strength values. The modelled specimen is loaded parallel to the direction of the fiber and the first fiber failure during the loading process occurs, when the load stress exceeds the tensile strength of the weakest fiber. Once the fibers begin to fail the released load of the broken fibers has to be redistributed to the intact fibers according to some specific interaction law between the fibers. A large amount of efforts have been devoted to understand the behavior of fiber bundles under

various load sharing conditions [6–24]. Based on a novel fiber bundle model introduced recently [25] a theoretical interpretation of the experimental results obtained for tension strength of clear wood parallel to fiber direction is presented. The macroscopic strength data are explained in terms of the damage process occurring on the micro-fiber level, i.e., on the level of the wood cells. In order to provide a quantitative characterization of the load redistribution among fibers a power law load-transfer function is proposed and its effective exponent is assessed.

In Section 2 a detailed description of the experimental procedure used for the uniaxial testing of wood specimens is presented. The experimental results are summarized in Section 3 followed by the presentation of the theoretical approaches in Sections 4 and 5.

2. Experiment description

The tested material was soft-wood of the species spruce (*picea abies*) being the most important wooden building material for load bearing timber structures in Europe. In order to investigate the size effect of tension strength parallel to fiber direction, two sets of specimens were manufactured distinguishing with respect to the cross-section by a factor of 10. Following the specimens with the smaller cross-section will be denoted “small” specimens and those with the large cross-section will be denoted “large” specimens. In order to minimize uncontrolled variability of material parameters of the natural material wood several aspects had to be taken care of:

- (1) All specimens were cut from one single log.
- (2) The specimens were selected to be free of macroscopic defects such as knots.
- (3) The most crucial parameter for the tension strength of the mainly unidirectional fiber composite wood is the angle between fiber direction, or longitudinal direction “L”, and applied tension load. Due to low tension strength perpendicular to fiber the strength off-axis decreases by about 50 percent at fiber deviations of 10° [26]. Within a typical rectangularly sawn scantling the deviation between nominal longitudinal direction of the stem and local fiber direction may vary considerably between 0° and about 15° . Whereas a non-destructive evaluation of the fiber deviation is technically quite demanding, the fracture surfaces of *splitted* wood indicate the fiber direction in a straightforward manner. Therefore the specimen raw material has been split to obtain straight grained wood pieces and the specimens were then cut parallel to the split surfaces.
- (4) As an additional measure of scatter reduction the specimens have been matched as twin-pairs consisting of one large and one small specimen each cut from adjacently located wood segments. Thereby each pair showed the highest possible conformity with respect to strength relevant parameters such as density or year ring width.

The specimen shape has been chosen with respect to three major aspects, being: (i) the anisotropy of the material with high tension strength parallel to fiber vs. low compression strength perpendicular to fiber direction; (ii) the low shear strength of the annual ring interface between high-density late wood and low-density early wood and;

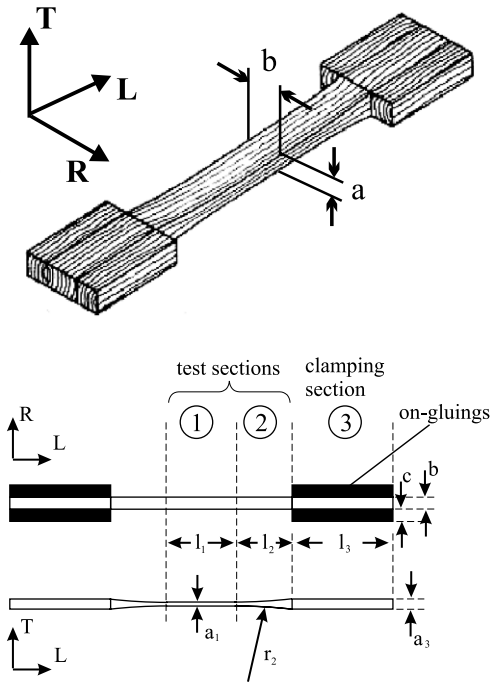


Fig. 1. Specimen geometry and the used notations.

Table 1
Nominal dimensions of the small and large tension specimens (in mm)

Nom. dim.	a_1	a_3	r_2	b	l_1	l_2	l_3	c	$A = a_1 b$
Small	2	5	200	6	35	27.5	50	6	12
Large	6	15	700	20	110	80	150	20	120

(iii) the necessity of scalability. Fig. 1 shows the employed specimen shape and the dimensional notations.

The dimensions of the small and large specimens are given in Table 1. The specimen shape is characterized by a rectangular cross-section with a shoulder shaped reduction of the thickness a_i parallel to the tangential growth direction T (following the annual rings).

In detail the specimen shape shows a straight section (1) of length l_1 with a constant minimal cross-section $a_1 b$, a curved shoulder section (2) of length l_2 and radius r_2 and, (3) the straight clamping section with cross section $a_3 b$ and length l_3 . The specimen's width b parallel to radial growth direction R (perpendicular to the annual rings) has been chosen constant in order to minimize shear and transverse tension stresses perpendicular to the weak annual ring interfaces.

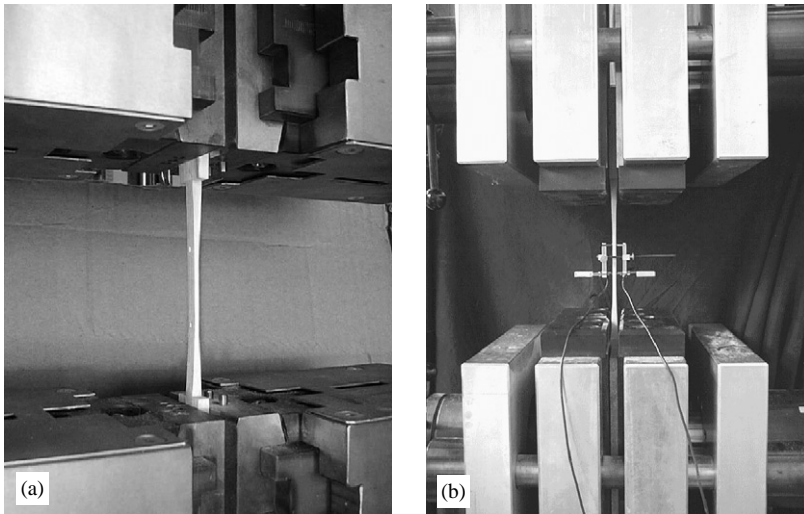


Fig. 2. Views of experimental setups for small (a) and large (b) tension specimens mounted in the different test machines.

In order to enlarge the clamping area in sections (3), thereby reducing the necessary compression stresses for load application in width direction, on-gluing of width c and depth a_3 were adhered both-sided to the ends of the specimens. All dimensions between the small and the large specimens were scaled by a factor of about $10^{1/2}$ in order to achieve geometrically similar shapes and a scale factor of 10 between the cross-sections of the small and the large specimens.

The load was applied to both, the small and large specimens by means of clamping. In case of the small specimens a screw clamp has been used with a nominally equally distributed compression stress at the clamping faces. In case of the large specimens hydraulic clamps were applied which allowed continuously decreasing compression stresses towards the edge of the on-gluing. Both clamping arrangements yield, compared to usual wedge type clamping devices, relatively smooth stress distributions at the transition from the clamping section to the test section.

The sets of small and large specimens consisted of 23 specimens each. The experiments were performed as stroke, (i.e., global deformation) controlled ramp-load tests with a constant cross-head displacement rate of the test machine. The stroke rate was chosen based on pre-testing of additional specimens such that fracture was obtained within 180 ± 60 s. In case of the small specimens the tests were conducted in a screw-driven test machine, whereas for the large specimens a servo-hydraulic type machine has been used. Fig. 2 shows photographs of a small and large specimen, installed in the respectively employed clamping arrangements of the different testing machines. In case of the large specimens, the mean strain of the straight section has been recorded with a strain gauge based extensometer, too Fig. 2b. However, as the strain was only measured for the large specimens the quantitative evaluation of the test results focuses solely on the strength results.

3. Experimental results

The fracture of the tension specimens occurred throughout within the test sections, i.e., predominantly in the straight section (1) and partly in the shoulder-shaped section (2). No failure occurred within the clamping section. Two typical views of broken small and large specimens are shown in Figs. 3a, b). The fracture surfaces were throughout influenced by the inhomogeneity of the annual rings: Distinct blunt tension ruptures can be observed in the early wood layers and then local shear failure planes along the early wood-late wood interfaces yielding pronouncedly stepped fracture surfaces. During the tension test it was not possible to follow the succession of fracture processes, however, quite often some cracking sound and dust presumably from a crack, yet not visible for blank eye could be observed prior to failure. Moreover, some of the stress–strain curves, recorded in case of the large specimens, showed pre-peak load drops with load recovery, which additionally indicated, that some kind of damage or crack evolution stop mechanism acted during loading. Fig. 4) shows a measured curve of global stress vs. global strain within the straight cross-section (1) of one large specimen exhibiting a pre-peak load drop. The ultimate failure occurred throughout as an unstable, brittle fracture. For all tests the maximum load was recorded and the strength was calculated on the basis of the individually measured minimal cross-sections. The mean values and standard deviations of the tension strength σ_c and the mean values of the effective cross-sections $A=a_1b$ are summarized in Table 2 separately for both test sets. The small specimens exhibited an 8.2 percent higher mean tension strength as compared to the large specimens. Thus, the results indicate a size effect of tension strength parallel to

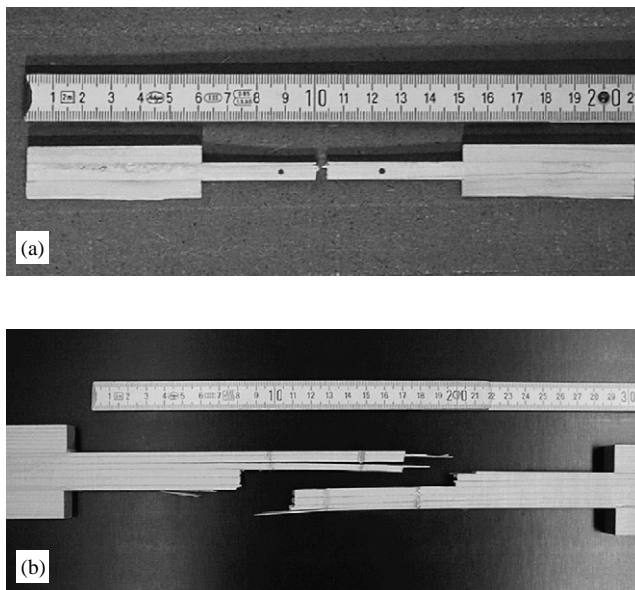


Fig. 3. Views of typical failure appearance of small (a) and large (b) specimens.

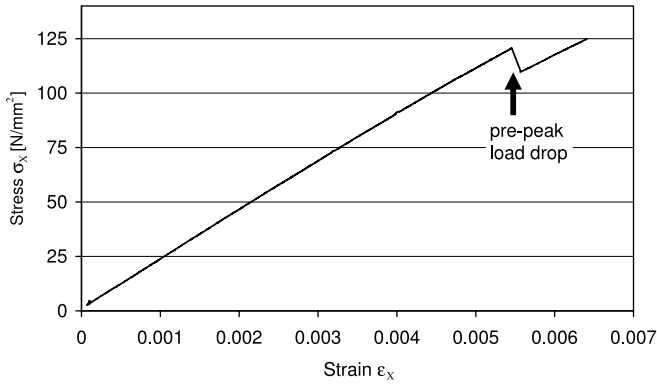


Fig. 4. Typical stress–strain behavior obtained for a large specimen.

Table 2
Summary of results of the tension tests

Specimen size	Cross-section (mm ²)	Number of Fibers	$\bar{\sigma}_c \pm \Delta\sigma_c$ (N/mm ²)	σ_0^b (N/mm ²)	ρ
Small	12.4	~ 5000	138.5 ± 18.7	146.2	8.3
Large	116.6	~ 50000	128.0 ± 13.6	134.0	10.3

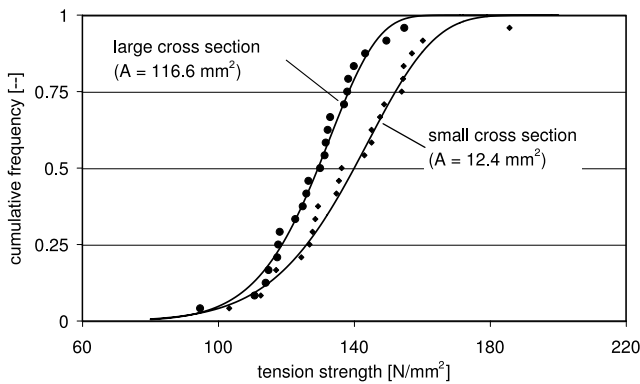


Fig. 5. Strength cumulative distribution from specimens with different sizes.

fiber of wood on the mean value level. However, also the scatter of the results is higher for the small specimens compared to the test set with the large cross-sections. Thus, the size effect seems to be smaller for the lower fractiles of the strength distribution.

The cumulative frequencies of both strength data sets are plotted in Fig. 5. Hereby the empiric cumulative frequency H_i of each individual strength value σ_c has been estimated based on ranking of the results in increasing order of the strength values

according to $H_i = n_i/(N + 1)$, whereby n_i and N denote the rank number and the total number of specimens in both samples, respectively. For both empiric sets of strength values a two-parameter Weibull distribution

$$P(\sigma_c) = 1 - \exp \left[- \left(\frac{\sigma_c}{\sigma_0^b} \right)^\rho \right] \quad (1)$$

has been fitted. In Eq. (1) quantity σ_0^b denotes the stress scale parameter and ρ is the Weibull shape parameter which characterizes the amount of disorder in the sample being determined by the coefficient of variation. The numerical result for the Weibull parameters, σ_0^b and ρ , obtained by least square fitting are given in (2); the respective cumulative distribution functions are plotted in Fig. 5 together with the empiric data.

4. Modelling of damage development

For a realistic modelling of the damage process of natural fiber composites under an uniaxial load, the local stress distribution would have to be calculated in the whole volume of the sample. Even limiting the number of independent variables needed to describe the internal microstructure of the specimen, an accurate prediction of the ultimate strength is a computationally demanding task. Hence, in general, the modelling of fiber composites is based on certain idealizations about the geometry of the fiber arrangement and the stress redistribution following fiber failures in the specimen. One of the most important type of models of fiber composites are the so-called fiber bundle models (FBM). In spite of their simplicity they capture most of the main aspects of material damage and failure, and hence, they have been successfully applied to the study of various kinds of composites. FBMs provided a deeper understanding of fracture processes and have served as a starting point for more complex models of fiber reinforced composites. If an uniaxial load is applied in the direction parallel to the fibers the actual composite stress σ_T can be obtained as $\sigma_T = \sigma_f A_f + (1 - A_f) \sigma_m$, where A_f denotes the fiber area fraction and σ_m is the usually small stress carried by the matrix. The matrix stress σ_m can normally be neglected in damage modelling since already at relatively low load levels, the matrix gets multiply cracked or yields plastically limiting its load bearing capacity. However, stress transfers between the fibers by the matrix action continues despite gradual damage so that it has a very important role in the load redistribution. In reconstituted artificial construction materials the range of load redistribution also called load sharing can be controlled by varying the properties of the matrix material and the fiber–matrix interface.

Two limiting or extreme cases of load redistribution can be distinguished: In the case of global load sharing (GLS), the load of a broken fiber is equally redistributed among all the unbroken fibers. This model is a mean field approximation where long range interactions are assumed among the elements of the system. For the case of high number of fibers it was proved [4] that strength σ_c of fiber bundles, when determined by global load sharing, is independent of the system size. Moreover, during the loading process the failure events are uncorrelated, resulting in a random spatial distribution of clusters of broken elements. In the case of local load sharing (LLS), being the other extreme,

it is assumed that the entire load of the broken fiber is taken by a local neighborhood of the failed element fiber. This case represents the short range interaction among fibers. The shape of the constitutive curve characterizing the macroscopic behavior of the system is the same as for GLS, but the maximum of the curve is shifted to lower stress values indicating a lower macroscopic strength and a more brittle behavior. The damage process is accompanied by a strong damage localization, i.e., the nucleated micro-cracks in the specimen tend to grow perpendicular to the load until a certain critical cluster size is reached. The critical cluster becomes unstable at an infinitesimal load increment and catastrophic failure occurs. Local load sharing implies that the global strength of samples decreases unlimited with the increase of the system size. In Ref. [17] a logarithmic size effect was revealed in a one dimension linear system of fibers loaded in parallel assuming that the load of broken fibers is taken by the two nearest intact fibers of the system.

The load redistribution in actual heterogeneous materials falls somewhere between the extremes of local and global load sharing. Usually there is an important fraction of stress redistributed to intact elements not located in the neighborhood of the failed ones, but also stress concentrations around broken fibers occur. During the last two decades, several studies on the strength distribution of composites were performed with FBMs [13,21–24], either based on analytic calculations or Monte Carlo simulations.

Now, if global load sharing is assumed in the case of small number of fibers, it can be shown analytically that the global strength of a bundle of Weibull fibers approximately follows a Weibull distribution, too [6,7,12,16]. The Weibull strength distribution then implies a decrease of the average strength according to a power law when the number of fibers is increased. Finally, approaching very large system sizes the strength distribution slowly converges to a normal distribution with a constant value of the average strength.

Contrary, when the load sharing mechanism is assumed to be completely localized, then the approximated strength distribution takes again the Weibull form, whereby the parameters, describing the macroscopic distribution, are different from the microscopic ones. The Weibull shape parameter of the bundle, ρ , is related to that of the single fibers as

$$\rho = N_c \rho_s, \quad (2)$$

where N_c denotes the size of the critical cluster of broken fibers. The Weibull distribution of global strength implies again a power law size dependence of the average strength which asymptotically turns into a slower logarithmic decrease [6,16].

A wood sample may be modelled by an array of parallel fibers arranged approximately on a regular square lattice. This is in agreement with the morphology of the real material at the micro-scale (see Fig. 6). The amount of matrix material between fibers is rather low, less than 1% of the total volume of the sample.

The macroscopic strength of fiber composites is mainly determined by the strength distribution of individual fibers and the interaction of fibers governing the load redistribution. Recently, the strength distribution of single wood fibers extracted from softwood materials has been studied extensively [27]. Experiments showed that the rupture of wood fibers is caused by the flaws of various sizes existing along fibers. The distribution of fiber strength values is controlled by the size distribution of flaws.

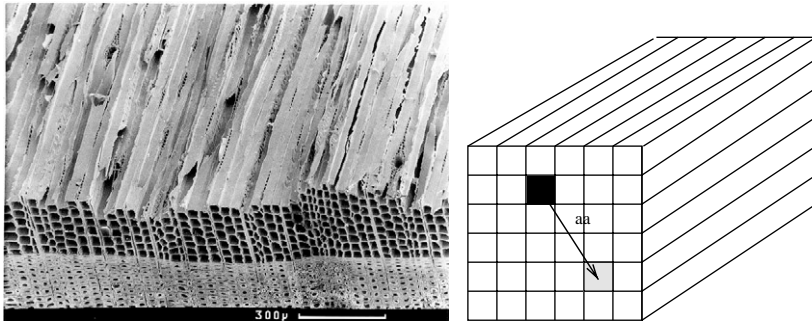


Fig. 6. The structure of softwood (left) and illustration of the model build-up (right). The wood fibers are arranged on a regular square lattice for which fiber bundle models can provide an adequate description.

It was found that the strength values σ_c of single wood fibers with a fixed length can be well described by a two-parameter Weibull distribution of the form of Eq. (1), with the stress scale parameter σ_0 and the Weibull shape parameter ρ_s , which characterizes the amount of disorder in single fibers. It was found that the value of ρ_s for single fibers always ranges from 1 to 2 indicating the presence of high disorder in wood fibers due to the pre-existing flaws [27].

In the above reported experiments on wood samples hardly any precursory breaking activity could be observed. The constitutive curves were practically linear up to the failure point and the final rupture occurred in a rather brittle manner suggesting a very localized load redistribution. The strong locality of load redistribution is further supported by the macroscopic Weibull shape parameters of $\rho \approx 8-10$, which are much larger than the corresponding range of single fibers acc. to [27]. Assuming completely local load sharing it follows from Eq. (2) that the size of the critical cluster in softwood is N_c in the range of 4–10; so when a cluster of N_c broken fibers is formed, the sample becomes unstable and fails abruptly. If the empiric data follow a Weibull distribution, which cannot be proved positively, the size effect can approximately be given in the power-law form $\sigma_0^b \sim N^{-1/\rho}$, where $\bar{\sigma}_c$ denotes the average strength of a sample of N fibers, which is in a reasonable agreement with the experimental results (see Table 2). The discrepancy between the calculated value of $(N_2/N_1)^{1/\rho} = 1.25$. and the value of $\sigma_{o1}^b/\sigma_{o2}^b = 1.08$. vs. the empiric data should result from the fact, that the extreme LLS case is approximate, but not an exact model for wood at tension loading parallel to fiber direction.

5. Fiber bundle model with variable range of interaction

In order to get a deeper insight into the damage process of wood at uniaxial loading in fiber direction a new fiber bundle model introduced recently [25] was applied. In the new model approach the interaction among fibers is modelled by an adjustable stress-transfer function. Varying the parameters of the model an interpolation is performed between the two limiting cases of load redistribution, the global and the local

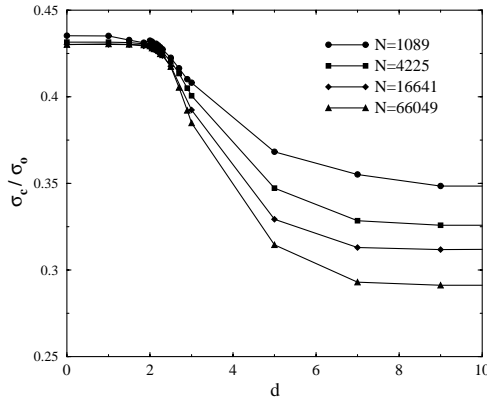


Fig. 7. Numerical estimates of ultimate strength of the fiber bundle material for different system sizes as a function of the effective range of interaction d [25].

load sharing schemes. The model is composed of N parallel fibers having statistically distributed strength drawn from a cumulative distribution function $P(\sigma/\sigma_0)$. Thus, to each fiber i a random strength value σ_{c_i-th} is assigned. All intact fibers have a nonzero probability of being affected by the ongoing damage process. Hereby the additional load received by an intact fiber i depends on its distance r_{ij} from fiber j which has failed. Elastic interaction is assumed between fibers such, that the additional load $\delta\sigma$ received by a fiber follows a power law form, i.e., in this discrete model the stress-transfer function $\delta\sigma(r_{ij}, d)$ takes the form

$$\delta\sigma(r_{ij}, d) \propto \frac{r_{ij}^{-d}}{Z}. \quad (3)$$

In Eq. (3) the quantity Z represents a normalization condition $Z = \sum_{i \in I} r_{ij}^{-d}$, the sum runs over the set I of all intact elements, whereby r_{ij} is the distance of fiber i to the rupture point (x_j, y_j) , i.e., $r_{ij} = \sqrt{(x_i - x_j)^2 + (y_i - y_j)^2}$ in a two-dimensional representation. Periodic boundary conditions are assumed so that the largest r_{ij} value conforms to $R_{\max} = (\sqrt{2}(S - 1))/2$, where S is the cross-sectional linear size of the square model $N = S \times S$. The geometrical model build-up is illustrated in Fig. 6). Quantity d is an adjustable model parameter, which determines the effective range of load redistribution. It is obvious from Eq. (3) that the limiting cases $d \rightarrow 0$ and ∞ represent the two extreme cases of load redistribution, being the global (GLS) and the local load sharing (LLS), respectively. Furthermore, intermediate values of d interpolate between the extreme load sharing cases. A comprehensive study of the general damage evolution in the framework of the model was carried out in Ref. [25]. The main results obtained are summarized in Figs. 7 and 8. In Fig. 7 the dependency of the average global strength of bundles on the system size, N , is presented for several values of d . Note that in every case the value of global strength is normalized by the characteristic strength value σ_0 , of the local strength distribution of single fibers. The numerical results confirm those obtained analytically in Refs. [14–16,6]. In Fig. 8

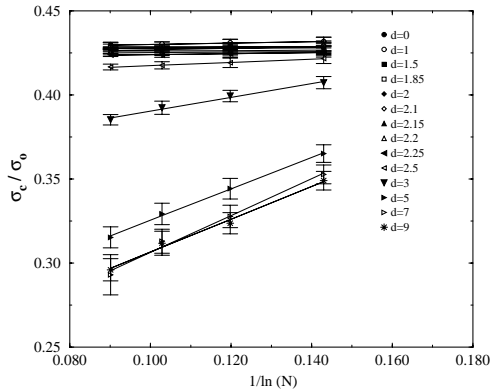


Fig. 8. Variation of the model strength with the system size (number of elements N) for several values of d [25].

the dependency of the global strength for different system sizes N as related to the load sharing exponent d is depicted. For small values of d ($d < 2.2$) the global strength of the bundle is approximately independent on the number of fibers, which is in agreement with the global load sharing approximation. However, the global strength of the system decreases with increasing system size for $d > 2.2$. In every case the results can be fitted by an inverse logarithmic law $\sigma_c/\sigma_0 \sim \alpha/\log N$ and only the slope of the curve, α , changes with the effective range of interaction determined by d . The logarithmic size effect is in agreement with the asymptotic size scaling of bundles with very localized interaction. In Section 3 a significant dependency of the average failure strength of the specimens on the size of their cross-section was obtained experimentally. Based on the empiric results, an estimate of an effective exponent d , characterizing the load redistribution in softwood, will be provided in the framework of the outlined model.

It is plausible that real materials are not characterized by the extreme cases of global or local load sharing. A real specimen with N fibers should have a normalized strength value $\sigma_c(N)/\sigma_0$ which falls between the bounds of the GLS and LLS approaches. The normalization constant σ_0 is the characteristic stress value of the cumulative strength distribution of single elements. As in the presented case σ_0 is unknown, it has been used as a free fit parameter.

For an estimation of upper and lower boundaries of σ_0 first the limits of GLS and LLS were calculated. Numerical results, using a cumulative Weibull distribution with the disorder parameter $\rho_s = 2$, are shown in the Figs. 7, 8. It can be seen that in the global case, due to the independence of the system size on the σ_c/σ_0 vs. $1/\log N$ graphic forwards a line parallel to the $1/\log N$ axis with $\sigma_c/\sigma_0 = (\rho_s e)^{-1/\rho_s}$. Note that given by Figs. 7 and 8 this value is $\sigma_c/\sigma_0 = 0.429$. This parallel line is the upper bound for the strength data of the test series with smaller number of fibers $N = 5000$. Using its corresponding strength value (shown in Table 2) yields the lower bound of $\sigma_0 = 322.8N/\text{mm}^2$.

Table 3

Load sharing parameters estimated from the strength values obtained from test samples with different sizes

Weibull disorder parameter	Weibull scaling parameter [N/mm ²]	Slope	Load-sharing parameter
$\rho_s = 1$	$384.7 < \sigma_0 < 520.1$	$0.8 < \alpha < 1.1$	$6 < d < 10$
$\rho_s = 2$	$322.8 < \sigma_0 < 426.5$	$0.9 < \alpha < 1.3$	$5 < d < 10$

In the same manner the limiting case of LLS ($d=9$), i.e., a line $\sigma_c/\sigma_0=0.971/\log N+0.21$, gives a lower bound of normalized strength, for the empiric test series with higher number of fibers $N = 50\,000$, and thereby yields the upper bound of $\sigma_0 = 426.5N/\text{mm}^2$.

In this way it is possible to fit the experimental results presented in Section 3 with the model using the fit parameter σ_0 . The slope of the fitted curves can be calculated, enabling a numerical estimation of the value d .

In Table 3 the results of the limit case considerations are compiled including the ranges of σ_0 , the derived slopes α and finally the resulting values for the load sharing exponent d . In the fitting procedure, two extreme values of the Weibull shape parameter ρ_s , previously determined by Thuvander et al., have been used [27]. Comparing the fitted values of α to the results of Ref. [25] it can be seen that the exponent characterize the load redistribution in wood in case of tension loading parallel to the fiber direction already falls in the regime where the behavior of the system can be well described by assuming almost completely localized load sharing. This result is in agreement with the general arguments of the previous section.

6. Conclusions

The size effect of tension strength of softwood loaded parallel to fiber direction has been assessed experimentally. The macroscopic constitutive behavior of the specimens was, as anticipated, rather brittle and the strength values showed a statistical variation which could be well fitted in terms of a Weibull distribution. It was revealed that the average strength is a decreasing function of the cross-sectional specimen size. In order to provide a theoretical interpretation of the experimental results with respect to the size effect and the modelling of the load sharing mechanism, the wood material was modelled as a natural fiber composite with extremely small volume fraction of matrix material. Comparing the strength distribution of single fibers and that of the macroscopic samples it was deduced that the load redistribution among wood fibers is short ranged giving rise to a low precursory activity preceding final failure and small clusters of broken fibers. For qualitative characterization of the load sharing it has been assumed that the load-transfer function has a power law form and its effective exponent has been estimated. The experimental and theoretical results are in satisfactory agreement.

Additional researches are needed in order to confirm the results in a more quantitative manner including experiments with intermediate size scales. Moreover, some aspects

of the damage evolution of wood at tension loading parallel to fiber are not yet well described by the used FBMs.

Acknowledgements

This work was essentially supported by the project SFB381 of the German Science Foundation (DFG) and by the NATO grant PST.CLG.977311. F. Kun acknowledges financial support of the Bólyai János Fellowship of the Hungarian Academy of Sciences and of the Research Contract FKFP 0118/2001 and T037212. Y.M. acknowledges financial support from the Secretaría de Estado de Educación y Universidades (Spain, SB2000-0357) and of the Spanish DGICYT Project BFM2002-01798.

References

- [1] J.D. Barrett, *Wood Fiber* 6 (2) (1974) 126.
- [2] J.D. Barrett, A.R. Fewell, Proceedings of the CIB-W18A Meeting, Lisbon, paper 23-10-3, 1990.
- [3] S. Aicher, G. Dill-Langer, W. Klöck, Proceedings of the CIB-W18A Meeting, Kyoto, paper 35-6-1, 2002.
- [4] H.E. Daniels, *Proc. Roy. Soc. London A* 183 (1945) 405.
- [5] B.D. Coleman, *J. Appl. Phys.* 28 (1957) 1058, 1065.
- [6] S.L. Phoenix, L. Tierney, *Eng. Fract. Mech.* 18 (1983) 193.
- [7] W.I. Newman, A.M. Gabrielov, T.A. Durand, S.L. Phoenix, D.L. Turcotte, *Physica D* 77 (1994) 200.
- [8] W.I. Newman, D.L. Turcotte, A.M. Gabrielov, *Phys. Rev. E* 52 (1995) 4827.
- [9] F. Kun, S. Zapperi, H.J. Herrmann, *Eur. Phys. J. B* 17 (2000) 269.
- [10] D. Sornette, *J. Phys. A* 22 (1989) L243.
- [11] D. Sornette, *J. Phys. I France* 2 (1992) 2089.
- [12] W.A. Curtin, *Phys. Rev. Lett.* 80 (1998) 1445.
- [13] S. Mahesh, I.J. Beyerlein, S.L. Phoenix, *Physica D* 133 (1999) 371.
- [14] A. Hansen, P.C. Hemmer, *Phys. Lett. A* 184 (1994) 394.
- [15] P.C. Hemmer, A. Hansen, *J. Appl. Mech.* 59 (1992) 909.
- [16] D.G. Harlow, *Proc. Roy. Soc. London A* 397 (1985) 211.
- [17] M. Kloster, A. Hansen, P.C. Hemmer, *Phys. Rev. E* 56 (1997) 2615.
- [18] R.C. Hidalgo, F. Kun, H.J. Herrmann, *Phys. Rev. E* 64 (2001) 066 122.
- [19] R.C. Hidalgo, F. Kun, H.J. Herrmann, *Phys. Rev. E* 65 (2002) 032 502.
- [20] D.G. Harlow, S.L. Phoenix, *J. Composite Mater.* 12 (1978) 195.
- [21] I.J. Beyerlein, S.L. Phoenix, *Eng. Fract. Mech.* 57 (1997) 241.
- [22] I.J. Beyerlein, S.L. Phoenix, *Eng. Fract. Mech.* 57 (1997) 267.
- [23] M. Ibnabdeljalil, W.A. Curtin, *Int. J. Solids Structures* 34 (1997) 2649.
- [24] M. Ibnabdeljalil, W.A. Curtin, *Acta Mater.* 45 (1997) 3641.
- [25] R.C. Hidalgo, Y. Moreno, F. Kun, H.J. Herrmann, *Phys. Rev. E* 65 (2002) 46 148.
- [26] F. Kollmann, *Technologie des Holzes und der Holzwerkstoffe*, Springer, Berlin, Heidelberg, New York, 1982.
- [27] Fredrik Thuvander, E. Kristofer Gamstedt, Per Ahlgren, *Nordic Pulp Paper Res.* 16 (2001) 46.